Experimental Analysis of the Effect of Metal Thickness on the Quality Factor in Integrated Spiral Inductors for RF ICs

Yun-Seok Choi and Jun-Bo Yoon, *Member, IEEE*

***Abstract*—The effect of metal thickness on the quality ($Q-$) factor of the integrated spiral inductor is investigated in this paper. The inductors with metal thicknesses of $5 \sim 22.5$ μm were fabricated on the standard silicon substrate of $1 \sim 30\ \Omega \cdot$ cm in resistivity by using thick-metal surface micromachining technology. The fabricated inductors were measured at GHz ranges to extract their major parameters (Q-factor, inductance, and resistance). From the experimental analysis assisted by FEM simulation, we first reported that the metal thickness' effect on the Q-factor strongly depends on the innermost turn diameter of the spiral inductor, so that it is possible to improve Q-factors further by increasing the metal thickness beyond 10 μm.**

***Index Terms*—Integrated micromachined inductor, metal thickness, micromachining, Q-factor, radio frequency (RF) ICs, resistance, RF MEMS.**

I. Introduction

RECENTLY, as the demand for smaller and more capable communication systems grows, radio frequency integrated circuits (RF ICs) require high performance passive components as an integrated form to reduce the total system size and assembly cost. Among the passive components, the inductor is a key in RF ICs since it is crucial for handling high-frequency signals. Because the performance of the inductor can determine that of RF ICs [1]–[4], an integrated inductor with high performance is vital. However, common integrated inductors in RF ICs have suffered from their poor performance stemming from the ohmic loss of the thin metal line in the standard CMOS process and the substrate loss in lossy silicon at high frequency. Increasing the metal thickness is the most efficient way currently known to increase the Q-factor in the Q-rising region where the frequency is below the maximum Q-factor point. From this perspective, several methods have been tested in order to increase metal thickness, such as using electroplating [5]–[7] or using multi metal layers [8]. Consequently, people want to know what the optimum metal thickness is, if any, since there are limiting factors like skin-depth and proximity (eddy current induced) effects in GHz ranges. So far, the effect of metal thickness to the Q-factor has been investigated mostly in a metal thickness range of a few microns [9], [10]. Some have reported that the saturation of the Q-factor occurs at a metal thickness of around ten microns [6], [11], where the results have been explained only by the skin-depth effect.

In this paper, inductors with a wide metal thickness range ($5 \sim 22.5$ μm) and an explicitly different innermost turn diameter (100 and 240 μm) have been fabricated and characterized to show that the metal thickness effect to the Q-factor is strongly dependent on the innermost turn diameter. This tendency has been interpreted by both skin-depth and proximity effects and verified by FEM simulation using HFSS. Consequently, we have shown that it is possible to improve the Q-factors further by increasing metal thickness beyond 10 μm.

II. Design and Fabrication

Two types of inductor were chosen for the experiment with the innermost turn diameter: D_{in}, of 240 μm for type 1 and 100 μm for type 2, respectively. The metal width (20 μm), space (15 μm), and outmost turn diameter (380 μm) have been equally used in type 1 and 2 inductors. The number of turns is 3 for type 1 and 5 for type 2. The expected inductances are 5 nH for type 1 and 6.5 nH for type 2, respectively, at a metal thickness of 10 μm [12].

Thick-metal surface micromachining technology was chosen for the fabrication of the inductors [7], [13] since the process consists of copper electroplating and thick photoresist lithography for fabricating very thick suspended metal line. The two inductor types were suspended at 25 μm on the oxide-passivated standard silicon substrate of $1 \sim 30\ \Omega \cdot$cm resistivity, where the oxide thickness was 7 μm.

III. Results and Discussion

The fabricated inductors were measured at the frequency range from 1 GHz to 5 GHz using the HP8510 network analyzer and the Cascade Microtech probe station with GSG probes and short-open-load-through (SOLT) calibration. Small pads (20×35 μm, 35 μm for skating side) for probing have been used so that the pad de-embedding has not been carried out. The Q-factor has been extracted from the measured 2-port Y parameters using the following equation, which is proportional to the frequency, f, and the series inductance, L_s,

Manuscript received November 6, 2003; revised December 4, 2003. This work was supported by the Ministry of Science and Technology, Korea, under a grant from the National Research Laboratory. The review of this letter was arranged by Editor K. De Meyer.

The authors are with the Division of Electrical Engineering, Department of Electrical Engineering and Computer Science, Korea Advanced Institute of Science and Technology (KAIST), Daejeon, 305-701, Republic of Korea (e-mail: gubk@iml.kaist.ac.kr; jbyoon@ee.kaist.ac.kr).

Digital Object Identifier 10.1109/LED.2003.822652

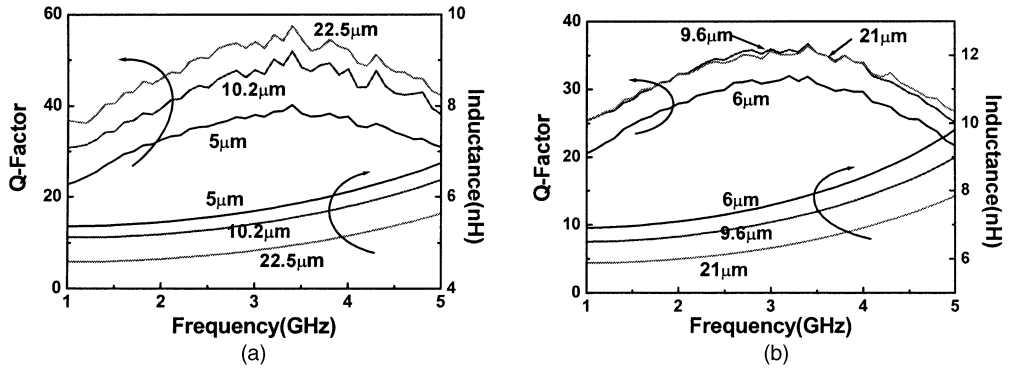

Fig. 1. Measured Q-factor and the inductance of the (a) type 1 inductor ($D_{in} = 240\ \mu$m) and type 2 inductor ($D_{in} = 100\ \mu$m) (the described numbers in the figures refer to the metal thickness).

and is inversely proportional to the series resistance, R_s, at the Q-rising frequency region

$$Q - factor = \frac{\mathrm{Im}\left[\frac{1}{Y_{11}}\right]}{\mathrm{Re}\left[\frac{1}{Y_{11}}\right]} \approx \frac{2\pi f \cdot L_s}{R_s}. \tag{1}$$

Fig. 1 shows the measured Q-factor and inductance of the type 1 and type 2 inductors; the Q-factor of the type 1 inductor (D_{in} of 240 μm) increases beyond the metal thickness of 10 μm, whereas that of the type 2 inductor (D_{in} of 100 μm) saturates at a metal thickness of around 10 μm. Note that the increase in metal thickness decreases inductance due to the reduction of the magnetic field outside of the metal line [9], [12].

The result shown in Fig. 1(a) is very interesting since previous works reported that the Q-factor did not increase beyond a metal thickness of 10 μm [6], [11], where the results were explained by a simple microstrip line model in which a metal ground exists at the backside of the substrate so that the current is confined at the bottom of the inductor line [9]. However, the microstrip line model is not suitable since the integrated inductor in RF ICs may not have the metal ground at the back side of the substrate [14], and even if it has the metal ground, the width of the inductor line is much smaller than the substrate thickness. In other words, the current in the inductor does not concentrate on the bottom of the metal line, but it can flow on the top and sidewall areas of the metal line as shown in Fig. 2 [15]. By thickening the metal, the Q-factor can be increased because of the reduced series resistance caused by the increased metal sidewall areas of current.

In order to verify the issue of the current flowing area, the series resistance R_s of the metal line at a Q-rising frequency has been calculated using the following equations in which all the effective cross-sectional areas of current are considered [15]

$$\lim_{f \to 0} R_{ac} = R_{dc} = \frac{1}{\sigma w t} \tag{2}$$

$$\lim_{f \to \infty} R_{ac} = kR_{hf} = k\frac{1}{2\sigma\delta(w+t)} \tag{3}$$

$$R_{ac} = \sqrt{R_{dc}^2 + (kR_{hf})^2} \tag{4}$$

where σ is the conductivity of copper, w is the width, t is the thickness, δ is the skin depth, and k is the correction factor (which is 1.2) for considering the edge behavior of the metal

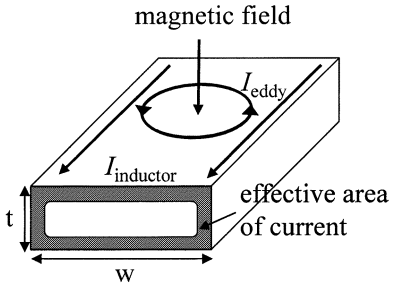

Fig. 2. Current distribution in the inductor to work with, which is affected by the skin and proximity effects.

line, respectively. The calculated R_s in Table I, which equals to R_{ac} in (4), also considered the contact resistance of each probe. We used GSG probes made of BeCu, which has been known to have a 0.1 Ω contact resistance when probed on a gold pad [16]. In spite of the fact that we used copper pads, we assumed contact resistance of 0.1 Ω for each pad since gold has a similar conductivity to that of copper. For the type 1 inductor, the calculated resistance matches well (less than 10% error) with the measured resistance showing that the current flows not only in the bottom, but also in the top and sidewall areas.

However, at the same time, Table I shows that the calculated R_s does not match with the measured resistance for the type 2 inductor. For the type 2 inductor with a metal thickness of over 10 μm, it can be observed that the measured resistance is not reduced as much as in the type 1 inductor and, hence, the Q-factor is saturated as shown in Fig. 1(b). Actually, this result is very similar to that of previous studies [6], [11].

The major difference between the type 1 and type 2 inductors is the innermost turn diameter, D_{in}. When D_{in} is small, which is the case for the type 2 inductor, the proximity effect becomes significant enough to induce eddy current in the metal line, as shown in Fig. 2 as well, consequently increasing the series resistance [17].

As the metal thickness increases from 5 to 10 μm, we can see that the increase of the effective thickness, which is calculated from [9] and shown in Table I, has contributed dominantly to the reduction of the series resistance for both type 1 and type 2 inductors. This is why the Q-factors of both type 1 and type 2 inductors have increased as the metal thickness increased from 5 to 10 μm. However, at the metal thickness increase from 10 to 20 μm, the effective thickness increase amount is negligible

TABLE I
SUMMARY OF THE INDUCTOR DIMENSIONS AND EXPERIMENTAL RESULTS AT 2 GHz $\left(R_s = \mathrm{Re}[-1/Y12], t_{\mathrm{eff}} = \delta \cdot (1 - e^{-t/2\delta})\right)$

	Type 1			Type 2		
Innermost turn diameter (D_{in})	240 μm			100 μm		
Metal thickness	5 μm	10.2 μm	22.5 μm	6 μm	11.2 μm	21 μm
Resistance, R_s @ 2 GHz	1.86Ω	1.58Ω	1.17Ω	2.49Ω	2.15Ω	1.97Ω
Calculated R_s @ 2GHz [15]	1.84Ω	1.45Ω	1.07Ω	2.1Ω	1.68Ω	1.3Ω
Inductance, L_s (nH)	5.4	5.2	4.6	7.1	6.7	6
Q-Factor @ 2GHz	32.6	39.5	46	27.9	32.3	32.2
Effective thickness, t_{eff}@2GHz [9]	1.26 μm	1.53 μm	1.59 μm	1.35 μm	1.54 μm	1.59 μm

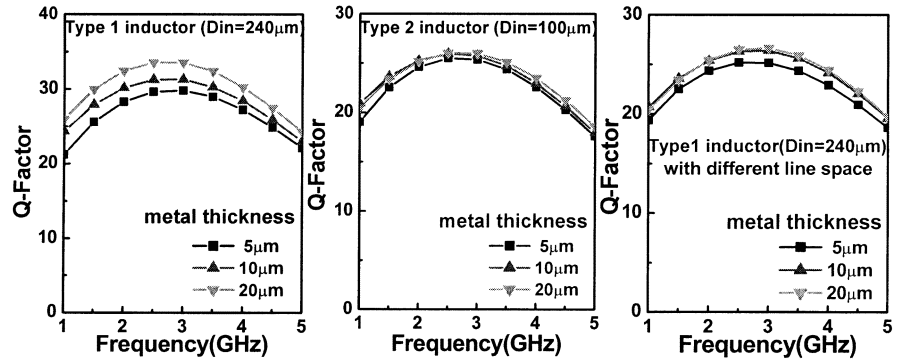

Fig. 3. FEM-simulated Q-factor of the (a) type 1 inductor, (b) type 2 inductor, and (c) type 1 inductor with narrower space ($15\ \mu\mathrm{m} \rightarrow 2\ \mu\mathrm{m}$).

as shown in Table I. Therefore, the resistance in this region becomes further reduced by the increase of sidewall height in the metal line, unless the proximity effect is significant. If the proximity effect becomes significant which is the case of the type 2 inductor, current in the metal line is confined on the one side of the conductor as shown in Fig. 2, and the resistance decrement is smaller than that of inductor having a negligible proximity effect. Therefore, the Q-factor of the type 2 inductor seems to be saturated in the region.

In order to verify the experimental results, an FEM simulation using commercial software of HFSS was conducted. Fig. 3(a) and (b) show the simulated result of inductor structures with the same geometry as measured from the type 1 and 2 inductors. The tendency of the Q-factor increment shown in the simulated results is very similar to that of the measured results in both type 1 and 2 inductors. Once we verified the tendency, we used FEM simulation further to investigate other geometrical dependency of the Q-factor. Fig. 3(c) shows the result for narrowing line space ($15\ \mu\mathrm{m} \rightarrow 2\ \mu\mathrm{m}$) from the type 1 inductor with the same line pitch of 35 μm. Contrary to the result in Fig. 3(a), we cannot observe a further increase of the Q-factor in the metal thickness increase from 10 to 20 μm. From this result, we can deduce that the increased proximity effect due to the narrower space suppressed Q-factor enhancement beyond metal thickness of 10 μm. For the case of varying the number of turns (3 to 5 for the type 1 inductor and 5 to 3 for the type 2 inductor), the tendency of the Q-factor variation was not significantly different from the original ones. Throughout the experimented and simulated results, it can be noted that the Q-factor enhancement as increasing metal thickness is dominantly determined by the proximity effect.

IV. CONCLUSION

From the experimental analysis of the micromachined inductors with a wide range of metal thicknesses and explicitly different innermost turn diameters, it was first reported that a different mechanism governs the Q-factor as the metal thickness increases, making it difficult to obtain any single optimum thickness for generic inductors. At the metal thickness range of 5 to 10 μm, the increase of the effective thickness of current mostly contributes to the Q-factor increase regardless of the innermost turn diameter. From the 10 to 20 μm metal thickness range, the proximity effect becomes dominant so that the innermost turn diameter determines whether or not the further increase of Q-factor is possible. Therefore, we have achieved substantial improvement in the Q-factors by increasing the metal thickness beyond 10 μm, using an inductor with large innermost turn diameter. Also, we have shown using FEM simulation that the line space plays a role when it gets smaller by increasing the proximity effect. These results can provide an important design guide for the fabrication of high performance integrated inductors for RF ICs.

ACKNOWLEDGMENT

The authors would like to thank Prof. E. Yoon and S. Hong for their support.

REFERENCES

[1] D. B. Lee, "A simple model of feedback oscillator noises spectrum," *Proc. IEEE*, vol. 54, pp. 329–330, Feb. 1966.

[2] E.-C. Park, Y.-S. Choi, J.-B. Yoon, S. Hong, and E. Yoon, "Fully integrated low phase-noise VCOs with on-chip MEMS inductors," *IEEE Trans. Microwave Theory Tech.*, vol. 51, pp. 289–296, Jan. 2003.

[3] R. Gupta and D. J. Allstot, "Fully monolithic CMOS RF power amplifiers: recent advances," *IEEE Commun. Mag.*, pp. 94–98, 1999.

[4] I. Aoki, S. D. Kee, D. B. Rutledge, and A. Hajimiri, "Fully integrated CMOS power amplifier design using the distributed active-transformer architecture," *IEEE J. Solid-State Circuits*, vol. 37, pp. 371–383, Mar. 2002.

[5] J. Y. Park and M. G. Allen, "High Q spiral-type microinductors on silicon substrates," *IEEE Trans. Magn.*, vol. 35, pp. 3544–3546, Sept. 1999.

[6] X. Huo, X. Chen, K. J. Chan, and P. C. H. Chan, "Silicon-based high-Q inductors incorporating electroplated copper and low-K BCB dielectric," *IEEE Electron Device Lett.*, vol. 23, pp. 520–522, Sept. 2002.

[7] J.-B. Yoon, Y.-S. Choi, B.-I. Kim, Y. Eo, and E. Yoon, "CMOS-compatible surface-micromachined suspended-spiral inductors for multi-GHz silicon RF ICs," *IEEE Electron Device Lett.*, vol. 23, pp. 591–593, Oct. 2002.

[8] J. N. Burghartz, M. Soyuer, K. A. Jenkins, and M. D. Hulvey, "High-Q inductors in standard silicon interconnect technology and its application to an integrated RF power amplifier," in *IEDM Tech. Dig.*, Dec. 1995, pp. 1015–1018.

[9] C. P. Yue and S. S. Wong, "Physical modeling of spiral inductors on silicon," *IEEE Trans. Electron Devices*, vol. 47, pp. 560–568, Mar. 2000.

[10] J. R. Long and M. A. Copeland, "The modeling, characterization, and design of monolithic inductors for silicon RF ICs," *IEEE J. Solid-State Circuits*, vol. 32, pp. 357–369, Mar. 1997.

[11] F. Ling, J. Song, T. Kamgaing, Y. Yang, W. Blood, M. Petras, and T. Myers, "Systematic analysis of inductors on silicon using EM simulations," in *Proc. Electronic Components and Technology Conf.*, 2002, pp. 484–489.

[12] H. M. Greenhouse, "Design of planar rectangular microelectronic inductors," *IEEE Trans. Parts, Hybrids, Packag.*, vol. PHP-10, pp. 101–109, June 1974.

[13] J.-B. Yoon, C.-H. Han, E. Yoon, and C.-K. Kim, "Novel two-step baking process for high-aspect-ratio photolithography with conventional positive thick photoresist," *Proc. SPIE*, vol. 3512, pp. 358–366, Sept. 1998.

[14] A. M. Niknejad and R. G. Meyer, *Design, Simulation and Applications of Inductors and Transformers for SI RF ICs*. Norwell, MA: Kluwer, 2000.

[15] R. F. Dana and Y. L. Chow, "The current distribution and AC resistance of a microstrip structure," *IEEE Trans. Microwave Theory Tech.*, vol. 38, pp. 1268–1277, Sept. 1990.

[16] J. L. Carbonero, G. Morin, and B. Cabon, "Comparison between beryllium-copper and tungsten high frequency air coplanar probes," in *Proc. IEEE MTT-S Int. Microwave Symp. Dig.*, 1995, pp. 1475–1478.

[17] J. Cranicnckx and M. S. J. Steyaert, "A 1.8-GHz low-phase-noise CMOS VCO using optimized hollow spiral inductors," *IEEE J. Solid-State Circuits*, vol. 32, pp. 736–744, May 1997.